CLINICAL ARTICLE

Histologic Observation and Significance of Sympathetic Nerve Fiber Distribution on Human Cervical Ligamentum Flavum

Xiaolin Wu, MD[1], Xiaoyan Wang, MD[1,2], Guoqing Zhang, MM[1], Zhu Guo, MD[1], Yan Wang, MD[1], Ronghuan Wang, MM[1], Hongfei Xiang, MD[1], Bohua Chen, MD[1]

[1]*Department of Orthopedics, The Affiliated Hospital of Qingdao University and* [2]*Department of Vascular Intervention, Qingdao Central Hospital, Qingdao, China*

Objective: To study the distribution of sympathetic nerves of the ligamentum flavum (LF), confirm its existence by histological observation and nuclear magnetic resonance spectroscopy, and analyze the relationship between sympathetic nerve fibers and the biomechanical structure of the LF.

Methods: Randomly controlled scientific research selected 15 cases of posterior surgery in the affiliated hospital of Qingdao University from January 2013 to December 2019. The average age was 67.5 ± 14.5 years old, eight males and seven females. The LF specimens (completely separated fresh tissue) of different segments ($C_{3\text{-}7}$) were taken during the operation. Two pages of LF specimens on the left and right sides of the same segment are randomly allocated by the pairing method for formalin fixation and cryopreservation in liquid nitrogen. LF specimens extracted from seven other adult cadaver specimens (average age at death of about 56.8 ± 4.0 years, three males and four females) were used as a control group; together with formalin- fixed specimens obtained during surgery, 3D slices were given layer by layer. The distribution of sympathetic nerves in different parts of the LF was analyzed by glyoxylic acid-induced biological monoamine fluorescent technique (SPG) and hematoxylin–eosin (HE) staining. Fifteen liquid nitrogen storage specimens were divided into the back of the LF and the spinal canal through frozen sections, and were analyzed by nuclear magnetic resonance spectroscopy-hydrogen spectrum (^{1}H -NMR) for neurotransmitters and neurometabolites.

Results: There were type C sympathetic nerve fibers in the LF, which were divided into linear shape (α) and wave shape (β). Experimental group (χ^2 = 1.705, $P > 0.05$) and control group (χ^2 = 0.879, $P > 0.05$) can detect no difference in fluorescence units. Nerve fiber transmitter metabolites choline (Cho), creator (Cr), γ-aminobutyric acid (GABA) also indicate that the sympathetic nerve is present in the LF. LF sympathetic nerve fibers were mainly distributed in the proximal spinal canal surface, nerve fibers on the medial belt (area II) were fewer than the lateral belt (area I) (W = 210, $P < 0.05$). The ^{1}HNMR spectrum of LF spinal canal PG / Cho (t = 8.721, $P < 0.05$), GABA (t = 16.01, $P < 0.05$) value increased, lactic acid (Lac) / Cr (t = 4.213, $P < 0.05$), Cho / Cr (t = 2.402, $P < 0.05$) value decreased, indicating that nerve fibers are actively metabolized on the surface of the spinal canal, mainly distributed in tube surface. βtype fibers were more often distributed around microvessels. A small amount of α type fibers went next to the vascular structures, while α type fibers and β type fibers go cross within LF. Two patients with vertebral artery dissection had no recurrence of sympathetic symptoms within a total of 12 follow-ups 2 years after discharge.

Address for correspondence *Bohua Chen, MD, Department of Orthopedics, The Affiliated Hospital of Qingdao University (East District), 59 Haier Road, Qingdao, Shandong, China 266003 Tel: +86-(0)13506483551; Email: bhchen@hotmail.com*

† Hongfei Xiang and Bohua Che Contributes equal.

Disclosure: The authors declare that they have no conflict of interest. This study was funded by the National Natural Science Foundation of China (81802190, 81772412), Shandong Medical and Health Technology Development Plan Project (2017WS033), and Young Taishan Scholars Program (tsqn201909190).

Received 5 January 2020; accepted 17 August 2020

Orthopaedic Surgery 2020;12:1811–1825 • DOI: 10.1111/os.12802

Conclusions: There are many sympathetic nerve fibers distributed on LF, and their distribution may be correlated with histological and mechanical characteristics of LF. It may also be the anatomical basis of cervical vertigo.

Key words: Cervical instability; Cervical spondylosis; Cervical vertigo; Ligamentum flavum; Sympathetic nerve fiber

Introduction

Recent studies on clinical practice experiences of cervical vertigo (CV) are also closely related to the classification of the cervical spondylosis. Traditional "CV" mainly refers to "cervical spondylotic arteriopathy" and "sympathetic cervical spondylosis," but the existence of "CV" is highly controversial[1].

Since Barre and Lieou put forward Barre–Lieou syndrome[2], the understanding of CV is developed from "due to vertebral basilar insufficiency (VBI) of vertebral artery caused by oppression of uncovertebral joint hyperplasia on lumens"[3] to the widely accepted theory of "symptoms caused by stimulations of uncovertebral joint osteophytes on sympathetic nerves of vertebral artery"[4], gradually formed doctrines represented by "mechanical compression of vertebral artery", "dysfunction of vertebral-basal artery circulation", "sympathetic nerve stimulation"[5–9], etc. But some clinical phenomenon are not well explained. However, it provides a new way of thinking about studies on sympathetic factors in ligament system around cervical canals and gradually reveals the important role of sympathetic factors in the causes of CV (Appendix S1–S3). As elaboration on the role of sympathetic factors in the causes of CV draws more and more attention, Yu Tengbo *et al.*[10] stated that there existed an obvious hemodynamic change of vertebral artery after stimulation on cervical sympathetic ganglion. They put forward that the sympathetic nerve in the neck was likely to be the main cause affecting hemodynamics, and constructed a "sympathetic nerve-hemodynamics-central nerve" reflex regulation mechanism. Anatomic studies also find that sinuvertebral nerves in human $C_{2\text{-}6}$ intervertebral foramens are from the corresponding meningeal branch of sympathetic ganglion. These nerves are distributed to the tissues in the spinal canal and around intervertebral foramen including the posterior longitudinal ligament (PLL)[11,12]. Experiment findings on human ligament confirm the distribution of sympathetic nerve fibers in PLL[13], intervertebral disc, articular process, joint capsule, and tissues around vertebral canal[14–16]. Confirmation on the existence of sympathetic nerve fibers and understanding on their distribution characteristics help to resolve the potential causes of the symptoms. This allows us to remark that the human cervical sympathetic peripheral nerves tend to distribute in anatomical structures related to cervical biomechanics with certain dynamic characteristics, while no nerve fibers are found in static bony structures such as vertebral body and vertebral arch. Ligamentum flavum (LF), as a special elastic protein connective tissue behind the canal to maintain the stability of the cervical spine, presents different biomechanical characteristics[17]. Therefore, followed by PLL, LF is selected as the research object, which can help to understand the distribution mode of sympathetic nerves under the background of biomechanics, thus the possible characteristics and significance can be assumed.

It has not been confirmed whether there are sympathetic nerve fibers in LF similar to those in PLL, intervertebral disc, and articular capsule. And it has not yet been reported about the existence of sympathetic nerves in human cervical LF and its characteristics. If the existence can be found, the universal distribution law of sympathetic nerve fibers in cervical soft tissues can be perfected, thus the theory of sympathetic nerve stimulation can be perfected.

The purpose of this study is to: (i) confirm the existence of sympathetic nerve fibers on the LF by glyoxylic acid-induced biological monoamine fluorescent technique (SPG) and nuclear magnetic resonance spectroscopy-hydrogen spectrum (^{1}H-NMR); (ii) by observing and comparing the characteristics of sympathetic nerve distribution in different regions and locations of the LF, speculate its possible pathophysiological significance; and (iii) combined with reports of clinically rare cases of "vertebral artery dissection," analyze the possible relationship and clinical significance of sympathetic nerve and CV.

Materials and Methods

Inclusion and Exclusion Criteria

Cervical LF tissues were obtained from all patients who underwent posterior cervical spine surgery in the affiliated hospital of Qingdao University from January 2013 to December 2019 and agreed to participate in the experiment. The average age was 67.5 ± 14.5 years (eight males and seven females). Other cadaver specimens were selected. The average age at death was about 56.8 ± 4.0 years (three males and four females). They were segregated into two groups: biopsy specimens and cadaveric specimens.

Inclusion criteria for the experimental and control groups.

Experimental group (biopsy specimens): (i) due to degeneration around the spinal canal and secondary changes, there were patients with symptoms or signs caused by oppression on spinal cord and blood vessels, etc ; (ii) in imaging examination (DR, CT, MRI), there were patients who objectively required posterior cervical spine surgery and (or) removal of all lamina and corresponding left and right two LF ; (iii) the left and right LF of the same segment are symmetrical, and the pairing is randomly divided into two groups: formalin fixation and liquid nitrogen preservation. Formalin-fixed specimens are equally divided into lateral belt (area I) and medial belt (area II) bands, and liquid nitrogen

preservation specimens are equally divided into the back of the LF and the LF spinal canal; (iv) sympathetic nerve fibers are widespread in the LF; and (v) randomized controlled study.

Control group (cadaver specimens): (i) adult cadaver without history of cervical vertebra disease who died of non-cervical vertebra diseases were selected. The bodies were treated by formalin for more than 1 year without obvious malformation, trauma, and degeneration excluded by the naked eye. All cadaver specimens meet all ethical requirements and retain the right of the donor's family to know; (ii) the LF specimens were cut into slices and treated with formalin in the experimental group; (iii) the staining result is compared with the experimental group; and (iv) there are sympathetic fibers in the LF.

Exclusion criteria for both groups: (i) those who do not meet the ethical requirements; (ii) injury, loss, asymmetry, developmental defect, ossification, tumor of the LF; (iii) patients who deny symptoms related to cervical spine; (iv) patients with endocrine and any metabolic diseases (including before birth); (v) the cadaver specimens were not treated with formalin; (vi) any patient who had undergone cervical surgery before obtaining the specimen; and (vii) incomplete imaging data.

Ethical Approval

The study was approved by the human ethics committee of the Affiliated Hospital of Qingdao University and the Ethics Office of Qingdao University. The ethics approval document number is QDFY-20-1013-11. All patients and cadaver family members provided written informed consent and the project was in accordance with the Helsinki Declaration of 1975.

Surgery Process

Anesthesia and Position

In patients undergoing posterior cervical spine surgery, a venous channel is established behind the patient's room to monitor body temperature, pulse, respiration, blood pressure, and blood oxygen saturation. Anesthesia induction: target-controlled infusion of 1.5–4.0 ug/mL propofol (Jiabo Pharmaceutical Co., Ltd., Guangzhou, China), 3–6 ng/mL sufentanil citrate (Renfu Pharmaceutical Co., Ltd., Yichang, China), after the patient's consciousness disappeared, intravenous infusion of 0.15 mg/kg cis atracurium (Hengrui Pharmaceutical Co., Ltd., Jiangsu, China). Intubation of video laryngoscope. During the operation, sevoflurane (Hengrui Pharmaceutical Co., Ltd., Shanghai, China) was maintained by inhalation, and cis-atracurium, sufentanil citrate, and propofol were used to maintain anesthesia. Position the body in the prone position, with the neck flexed forward, and tape the shoulders toward the foot. The upper extremities were fixed posteriorly and the cranial part was fixed in a "head-to-foot 15°position," fully revealing the posterior part of the neck (Fig. 1E); the autopsy operation was the same as the conventional operation group except that there was no anesthesia and disinfection procedures.

Approach and Exposure

Preoperative imaging data comprehensively determine the "post-cervical vertebral laminectomy and screw fixation" method (Fig. 1A–C): take a mid-posterior cervical incision, cut the skin, subcutaneous and deep fascia layer by layer, and cut the ligament of the item. A blunt dissection of the paravertebral muscles along the midline reveals the spinous processes, lamina, facet joints, and transverse processes that require decompression. The Addison's retractor is used to retract the bilateral paravertebral muscles. Drive appropriate pedicle screws or lateral mass screws on both sides (Fig. 1F, G), and drill a longitudinal bone groove with a width of about 2.5 mm along the medial edge of the bilateral facet joint. The bottom of the bone groove is deep to the lower cortex (inner plate) of the lamina. Lamina bone forceps stealthly bite off the inner cortical bone, the nerve peeler carefully peels the adhesion of the outer edge of the LF and the dura mater, and both sides simultaneously expose the decompression spinal canal[18] of the total lamina, and the lamina is combined with the continuous LF. The specimen is submitted for inspection (Fig. 1D). Flush the incision and fix the longitudinal rod. The operation was completed after further treatment of the wound.

Rare Case Studies

In this study, two relatively rare patients with "vertebral artery dissection" were both from the same research unit and were admitted to the emergency department within the time limit (Figs 2 and 3). The medical history and case data were provided by the neurointerventionist with the patients' knowledge and consent. The symptoms of "sympathetic excitement," mainly "dizziness," were treated with antiplatelet and anticoagulant in emergency, and sympathetic symptoms were significantly improved. The treatment experience of this rare case provides a certain degree of pathophysiology for this case illustration. After the patients were discharged from the hospital, they were followed up for "sympathetic symptoms" once every 2 months for 2 years, and the recurrence of symptoms and subjective feelings were recorded.

Paraffin Section

During paraffin embedding[19], each specimen was divided into two areas (lateral, area I; medial, area II) with equal width according to the width of LF. Specimens were given 3D sectioning in a sequence of coronal section, sagittal section, and axial section (to ensure the largest observation area), namely serial section along and vertically to the direction of ligament fibers. Coronary section was positive and negative sections of deep and shallow LF; sagittal sections were divided into area I and II; and axial sections were area far away from attachment points of LF which were of obvious characteristics. Number of sections in each direction was

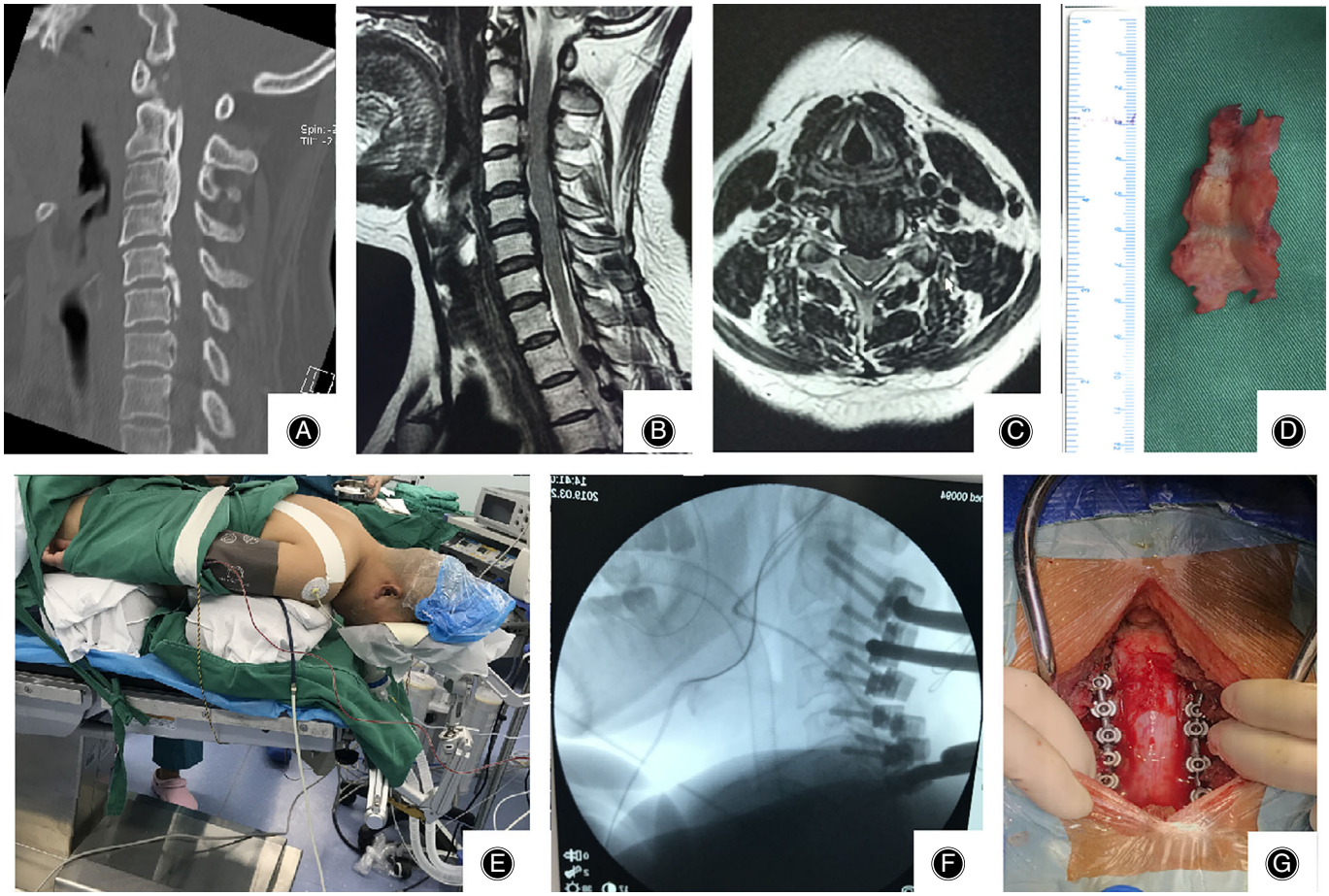

Fig. 1 Female, 50 years old, "cervical spinal stenosis" patient: (A) Preoperative CT showed PLL $C_{2\text{-}7}$ posterior longitudinal ligament ossification (OPLL), developmental cervical spinal stenosis; (B) Preoperative nuclear magnetic resonance showed $C_{3\text{-}5}$ segment cervical spinal cord pressure; (C) MRI $C_{3/4}$ level T2WI axial image, showing that the lamina ligament attached to the back of the lamina is normal in shape; (D) The $C_{3\text{-}5}$ intact whole lamina-LF complex removed during the operation is the same after the ligament is peeled off, segmental LF specimens were fixed with formalin and preserved with liquid nitrogen; (E) The "head-to-foot sole 15°" posterior cervical surgery posture; (F) Pedicle-side block screw fixation after total laminectomy during operation; (G) Cervical spinal cord decompression after total laminectomy and fixation.

not less than five, and the thickness was controlled in 3–4 μm.

Observation of Results and Data Processing

All sections were detected by fluorescence microscope (Olympus, Tokyo, Japan). Tuning excitation wavelength was 410 nm. Microscope was performed on sections of different areas and space directions at high magnification (×400) under fluorescence conditions. And image analysis software Image-Pro Plus 9.0 (Media Cybernetics Inc., Rockville, Maryland, USA) was supplemented for qualitative analysis. In all view fields, dotted or linear fluorescence was considered as a valid counting unit to record the detection value of each section, and each section with effective fluorescent unit of fixed area >5 was a positive microscope result. Corresponding data were measured and recorded for statistical processing.

Morphological Measurement of Sympathetic Nerve Fiber Fluorescence Imaging

Fluorescent units of the two types of nerve fibers from 20 cases of coronary or axial sections with positive fluorescence expression were randomly selected. Based on image measurement analysis, width value of fluorescence units of each section were recorded.

NMR ^1H Spectrum Detection

Biopsy and cadaver groups of LF tissue specimens were extracted from liquid nitrogen, each case in the group (a total of 15 cases) was about 250 mg, and the tissue slicer "scale equally" was used to quickly cut deep tissue (spine canal) and shallow layer (back) of tissue at −25°C. Add 50% acetonitrile (CH_3CN) (Honeywell Burdick & Jackson Inc., Michigan, USA) and 50% H_2O, make a homogenate in an ice bath, centrifuge at 50°C for 20 min at 4°C, and treat the

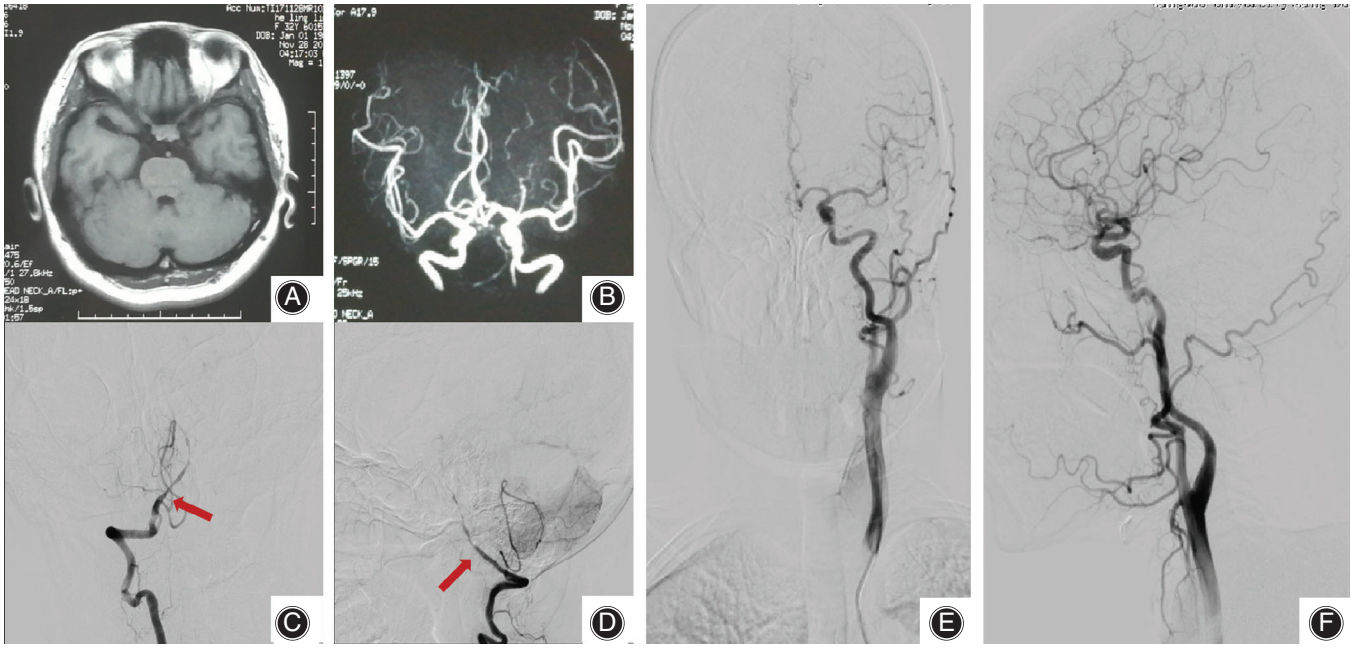

Fig. 2 Female, 32 years old, "vertebral artery dissection" patient: (A) Admission cranial MRI examination T1WI showed normal cerebellum and intracranial structure; (B) Admission MRA examination showed normal vertebral-basal artery circulation and vascular structure; (C) Emergency DSA examination showed vertebral artery V4 segment vascular dissection (anteroposterior imaging); (D) Vertebral artery V4 segment vascular dissection combined with stenosis (lateral imaging); (E) Follow-up after anticoagulation and antiplatelet therapy, and then follow-up DSA examination shows stable dissection (anteroposterior imaging); (F) Follow-up DSA (lateral imaging).

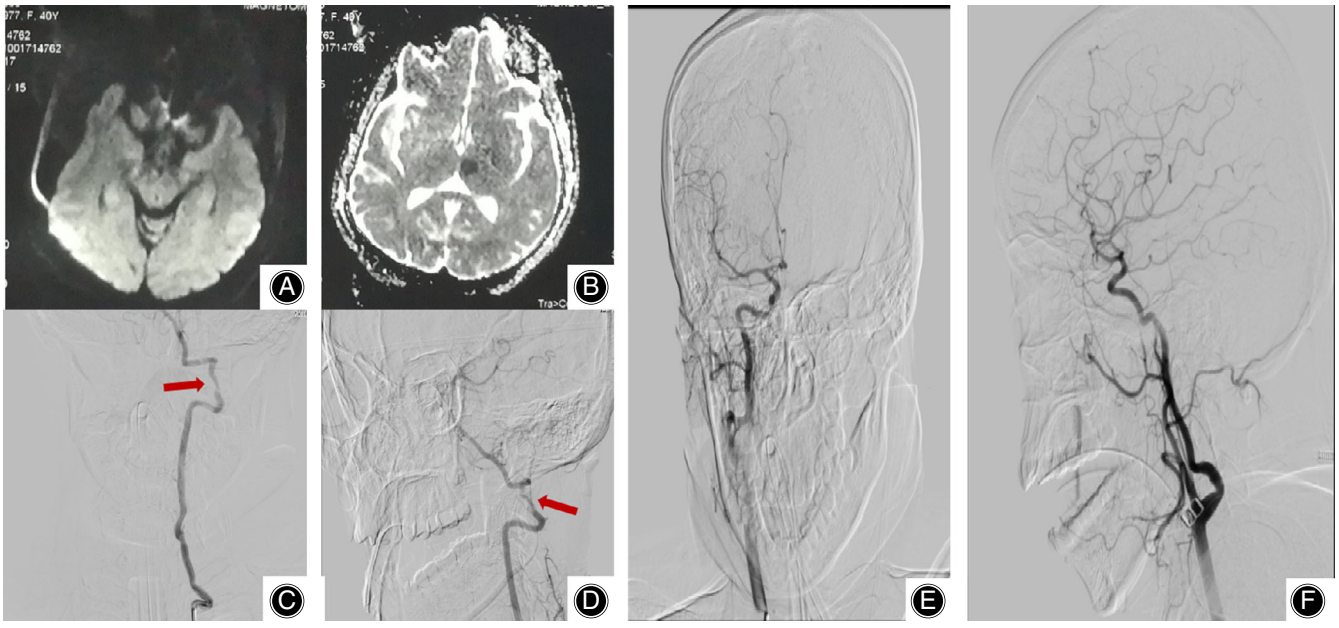

Fig. 3 Female, 39 years old, "vertebral artery dissection" patient: (A) Admitted cranial diffusion-weighted imaging (DWI) examination showed normal cerebellum and intracranial structure; (B) Apparent diffusion coefficient (ADC) showed normal cerebral nerve structure and function, excluding space-occupying lesions; (C) Emergency DSA examination showed vertebral artery V3 segment vascular dissection (anteroposterior imaging); (D) Vertebral artery V3 segment vascular dissection with stenosis (lateral imaging); (E) Follow-up after anticoagulation therapy and then DSA examination show that the dissection is stable (anteroposterior imaging), (F) Follow-up DSA (lateral imaging).

supernatant and precipitate separately. Take the supernatant after centrifugation, blow off CH_3CN with nitrogen, add it to the freeze dryer, and freeze-dry for 5 h. Take out the dried sample, add 500 uL of deuterium oxide (D_2O) (Nanjing Chemical Reagent Co., Ltd., Nanjing, China) and 100 uL of 10% TSP. After mixing, centrifuge at 14,000 × *g* for 20 min (to remove the precipitated particles of the tissue in the solution), and take 550 uL of the supernatant. The precipitate after centrifugation was taken, extracted with 2 mL of a solution of 75% trichloromethane ($CHCl_3$) (Sigma-Aldrich LLC., Shanghai, China) and 25% methanol (CH_3OH) (Jiexing Biotechnology Co., Ltd., Shanghai, China) and centrifuged at 50°C for 15 min at 4°C. Take the supernatant and blow off CH_3CN with nitrogen, put it in a freeze dryer and freeze-dry for 5 h. Take out the dried sample, add 600 μL of 75% chloroform-D ($CDCl_3$) (Estop Inc., Wuhan, China) / 25% methanol-D4 (CD_3OD) (Estop Inc., Wuhan, China), leave it for 10 to 15 minutes, and centrifuge at 14,000 × *g* for 10 min. Take the supernatant and mix with the supernatant. The samples were transferred into 3 mm nuclear magnetic tubes, and the three-axis gradient was used in a Bruker 500 MHz NMR spectrometer (Bruker Inc., Belgium, Germany) using a probe (ID500-5EB, Nalorac cryogenic Co., Ltd., USA) to obtain ^1H spectra of tissue samples. The jMRUI 6.0 software[20] (Stephen Provencher Inc., Canada) was used to remove water. Combine and identify substances for each peak integration (Fig. 4). Integrate the peak values of five metabolites: choline (cho), creator (Cr), proteoglycn N-Acetyl resonance (PG), γ-aminobutyric Acid (GABA), and lactate (Lac). The Lac / Cr, PG / Cho, Cho / Cr, GABA values are compared.

Statistical Analysis

The obtained data should be analyzed with SPSS 25.0 (IBM, USA) statistical software package, count the number of slices showing fluorescence units, and calculate the ratio with the total number of slices. The positive rate value of the obtained fluorescence slice is expressed as a percentage (%). Measure the fluorescence unit fluorescence photometric value on different slices, and take the average value for multiple measurements. The measurement data is described by ($x \pm s$). The distribution of fluorescence photometric values lateral and medial belt of the LF was tested by Wilcoxn rank sum test of two pairs of samples. NMR data is directly integrated by the jMRUI 6.0 software to obtain the absolute quantitative value. The fluorescence positive rate of each slice, the fluorescence positive rate of the two groups of specimens, and the distribution of nerve fiber types at different locations of the LF were compared using the chi-square test, and the comparison of the ratios of metabolites in the NMR ^1H-spectrum was by *t* test; $P < 0.05$ was considered statistically significant. GraphPad Prism 8 (GraphPad Software, USA) was used to draw the fluorescence photometric curve.

Outcome Measures

Biological Monoamine Fluorescent (SPG)

Glyoxylic acid can react with amine groups of catecholamines in sympathetic nerve fibers to mark neurotransmitter biomolecules. After staining sympathetic nerve fibers of different directions, spot or linear fluorescence expression can be observed, and its count value is the fluorescence value. The ratio of the fluorescence expression on the statistical section is defined as the fluorescence positive rate. The application software measures the brightness of the fluorescence unit to obtain the fluorescence photometric value. These can directly reflect the shape and density of sympathetic nerve fibers in tissues.

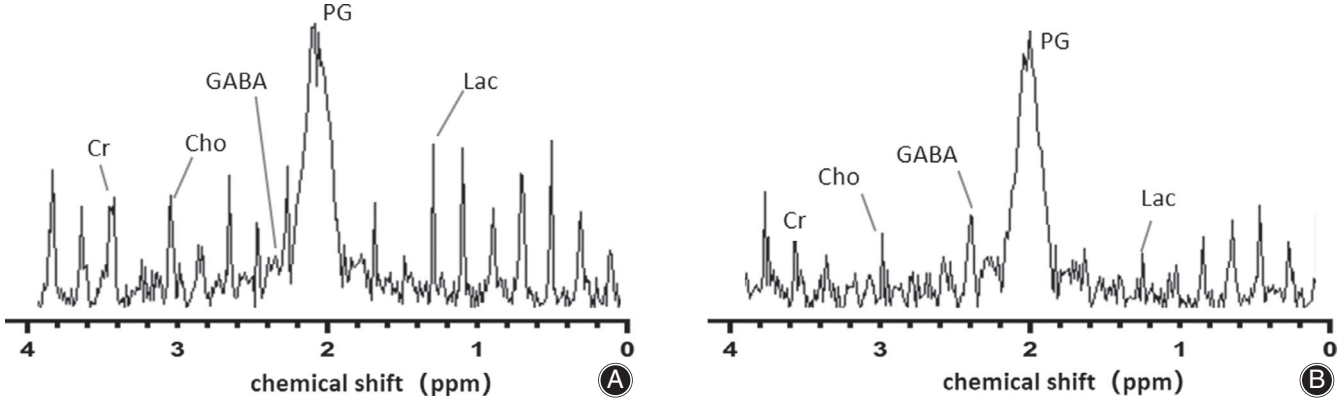

Fig. 4 (A) ^1H-NMR spectrum of the tissue of the LF back, showing that the content of choline (Cho) and creator (Cr) of peripheral neurotransmitter metabolites is significantly lower than that of the spinal canal, while proteoglycn N-Acetyl resonance (PG) and γ-aminobutyric Acid (GABA) and lactate (Lac), as metabolites of isolated tissue, were not different from those of the LF of the spinal canal; (B) ^1H-NMR spectrum of the LF of the spinal canal, with PG as the main constituent, Cho and Cr representing metabolites of peripheral neurotransmitters, and increased metabolism in isolated specimens GABA.

Classification of Sympathetic Nerve Fiber Morphology

C-type sympathetic nerve is a kind of post-ganglionic adrenergic non-myelinated nerve fiber. The nerve fiber diameter is 0.7–1.2 um and belongs to the sensory nerve. It is currently found to be linear (αtype) and wavy (βtype). Morphological measurement mainly depends on SPG. The method of staining is directly measured according to the fluorescent expression form. The unit is expressed in um. The different characteristics of its different types of distribution may have important significance for the study of the cause of cervical vertigo.

NMR ^{1}H Spectrum Metabolites

NMR ^{1}H spectroscopy is an application of the NMR effect of hydrogen-1 in molecules to NMR spectroscopy. The NMR ^{1}H spectra of most bioorganic compounds are characterized by chemical shifts and spin coupling between +9 and 0 ppm. The integral curve of the proton peak reflects its abundance.

Metabolite Parameters

Several of the most abundant and metabolic substances related to nerve structure in this study are: Cho, a choline-containing complex, including phosphocholine and phosphoacetylcholine, is a precursor of the important neurotransmitter acetylcholine and its main peak is located at 2.90–3.25 ppm; Cr, including creatine and creatine phosphate, is related to energy metabolism and is a reserve form of high-energy phosphate, and its main peak is located at 3.03–3.6 ppm; PG is used to represent the main proteoglycans and collagen ingredients, and assists in understanding the degree of decomposition of proteoglycan matrix and collagen matrix, with its main peak located at 2.04–2.10 ppm; GABA, is the main inhibitory neurotransmitter in the central nervous system, the expression is not high in the peripheral nerve but in the adrenergic nerve transmitters co-exist, the main peak is located at 2.35–3.02 ppm multiple peaks and often overlapps with other substances, the peak at 2.35–2.40 ppm is used as the index peak; Lac is an indicator of ischemic injury, is often used as the reference substance for the comparison of spectral substances, and is located at 1.31 ppm.

Ratio of Metabolite Parameters

The rate of metabolic parameters are as follows: Lac/Cr, mainly represents the degree of tissue ischemia and hypoxia, objectively reflects the distribution of microvessels and metabolite changes after nerve fiber destruction; PG/Cho, used to represent the relationship between nerve fiber and proteoglycan, its objective is to describe the structural distribution of sympathetic nerves in the ligamentum flavum; Cho/Cr is related to the activity of neurotransmitter metabolism. As Cr increases, neurotransmitters are also consumed.

Results

General Results

In the fifteen cases of posterior surgery, the average age was 67.5 ± 14.5 years old, eight males and seven females. There were also seven adult cadaver specimens, the average age at death was about 56.8 ± 4.0 years, withthree males and four females.

Histological Observation on Sympathetic Nerve Fibers of Sections of Human Cervical Ligamentum Flavum (LF) at Different Directions

Sympathetic nerve fibers were scattered among thick LF elastic fibers, which was observed on a shallow area of LF (area I and II), namely sections near surface of spinal canal (Fig. 5A). Most of the nerve fibers were distributed vertically,

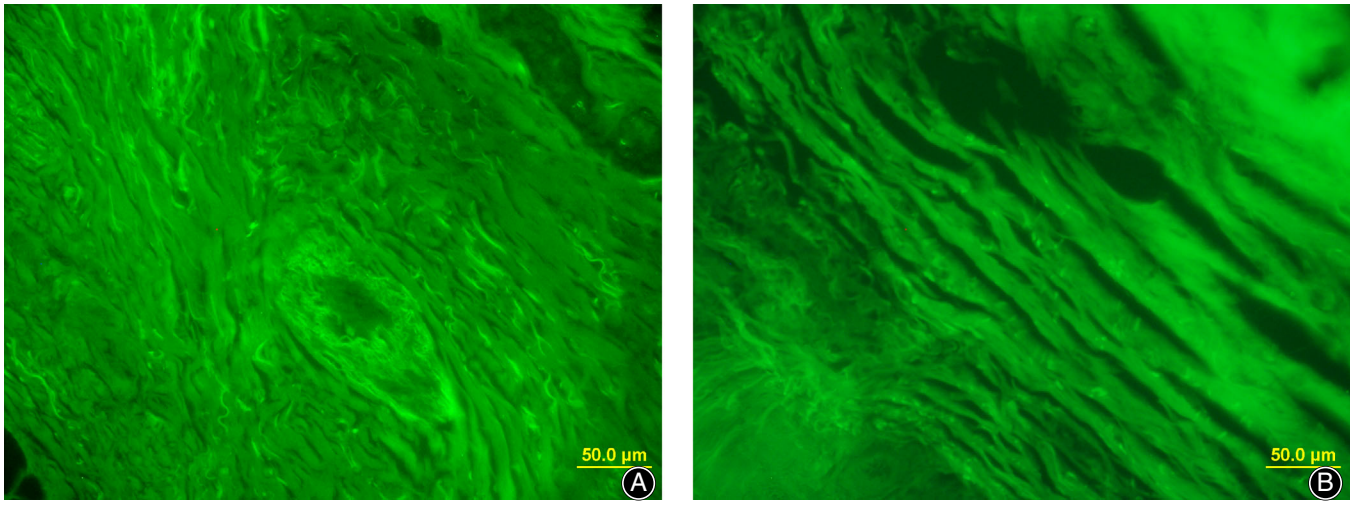

Fig. 5 (A) Linear and wavy sympathetic nerve fibers with yellow-green fluorescence among the LF nerves were observed in sections near surface of spinal canal under high-power microscopy (×400); (B) Linear and wavy sympathetic nerve fibers with yellow-green fluorescence among the LF that near the zygopophysis, nerves were observed in sections of different directions (×400).

with the fibers and some linear fibers moving out from the fiber bundle in a cluster shape; these were associated with sympathetic nerve fibers in joint capsule near the zygopophysis (Fig. 5B). Serial section was adopted on the same specimen and the adjacent slices with high quality were selected for HE staining and SPG staining, and the results were observed and analyzed. Some perforator vessels of arterioles were among LF fiber bundle. Under HE staining, arteriole structure in area I mainly went along LF fiber (Fig. 6A) while rarely went perpendicularly to the fibers; whereas in area II, different amounts of veins without arteriole structure went perpendicularly to the ligament fibers (Fig. 6C). A small amount of blood cells can be observed in lumens of axial sections in area I under fluorescent staining, and clear arterial wall can also be observed; and, in addition, adipocyte cells were scattered in epidural adipose tissue and lateral ligament (Fig. 6B,D), which were in line with the anatomic performances of the peripheral LF[7]. Some short and wavy short nerve fibers were around the outer wall of the vessel cavity. These nerve fibers were not concentrated in a section but scattered around (Fig. 7A–C).

Linear sympathetic nerve fibers that went out from LF in clusters can be observed on coronary sections of area I, mixed with some wavy sympathetic nerve fibers (Fig. 7D).

Dotted fluorescent units of sympathetic nerve fibers can be observed on coronary section of LF in area II (Fig. 5B), which went through elastic fibers. And elastic fibers on LF can be observed by HE staining.

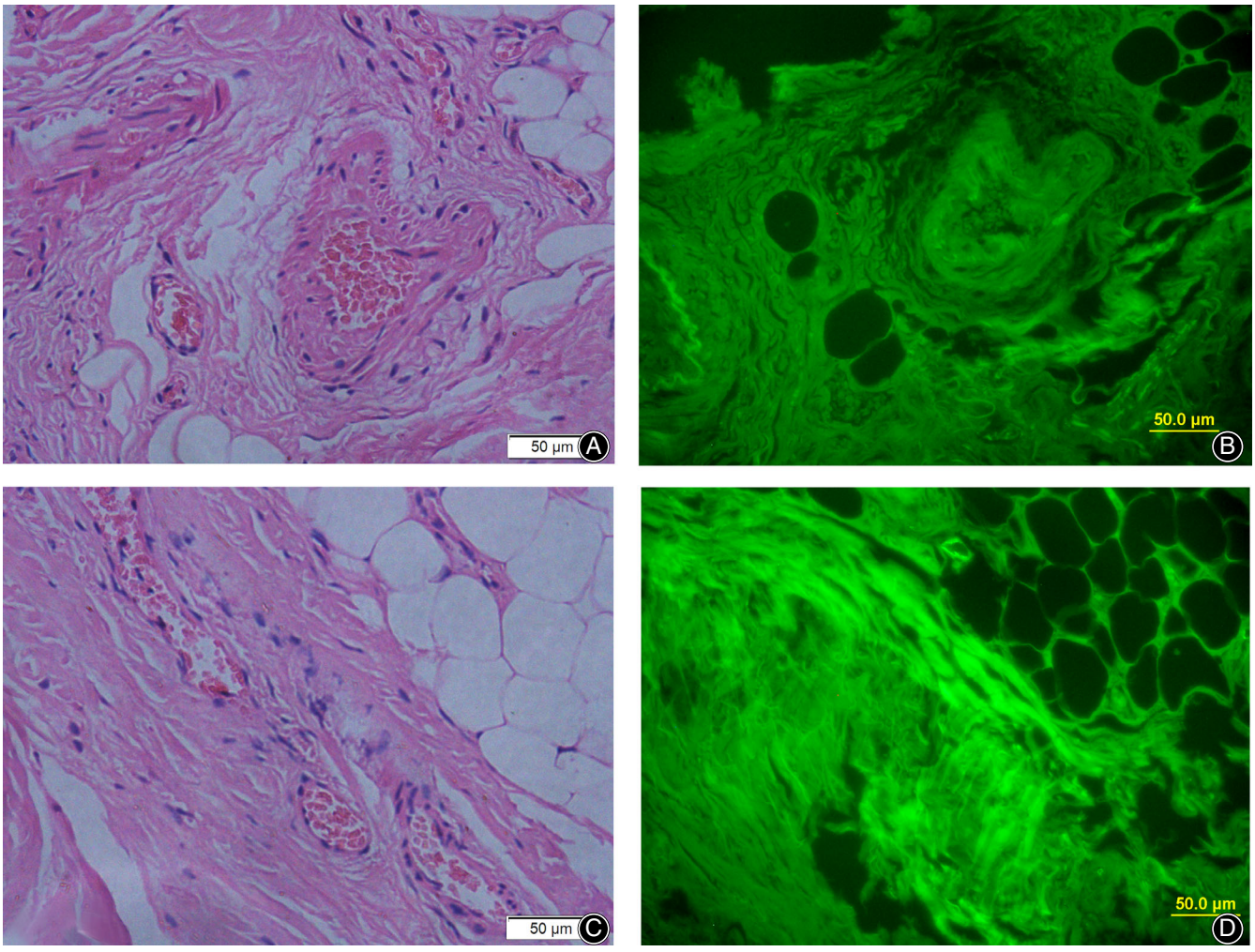

Fig. 6 (A) Area I of the LF spinal cannal was stained with HE, and the arterioles traveled along the elastic fibers and distributed on the lateral and spinal canal surface of FL (HE×400); (B) Sympathetic nerve fibers with aggregation of vessels (arteriole) were observed in sequential SPG stained sections in the same way as in Fig. 6A (SPG × 400); (C) Area II of the FL, different amounts of veins without arteriole structure went perpendicularly to the ligament fibers (HE×400); (D) Sympathetic nerve fibers with aggregation of vessels (venule) were observed in sequential SPG stained sections in the same way as in Fig. 6C (SPG × 400).

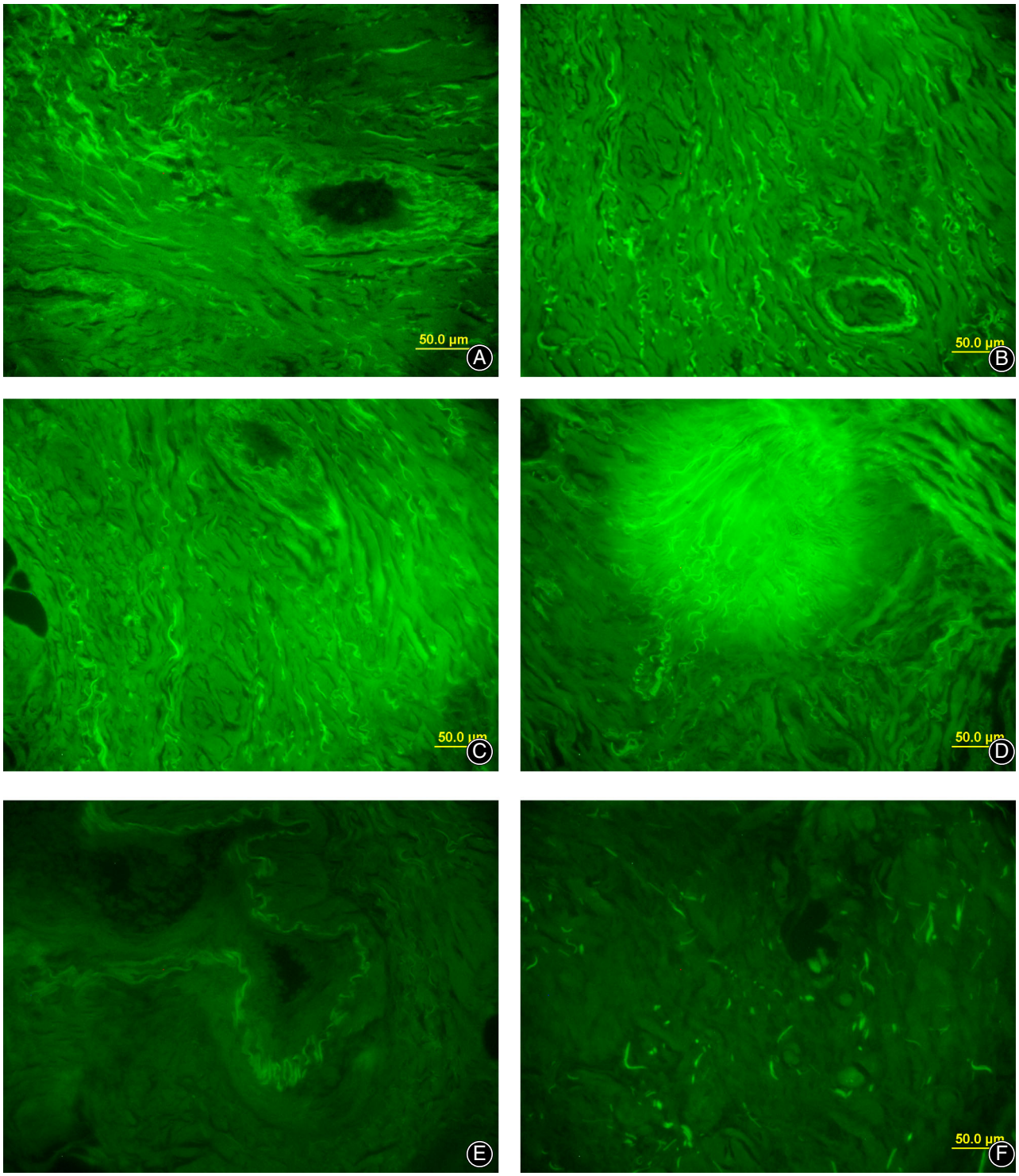

Fig. 7 (A) Fig. 8. Comparative statistics of the expression of sympathetic nerve fluorescence in the LF area I and II, more and denser sympathetic nerve fibers were distributed in area I compared to area II. Fluorescent expression of linear (α) and wavy (β) sympathetic nerve fibers distributed along the venules of the FL (SPG × 400). It can be seen that the two types of nerve fibers have different width; (B) Fluorescent expression of wavy (β) sympathetic nerve fibers distributed along elastic fiber bundles of the FL (SPG × 400); (C) Fluorescent expression of linear (α) and wavy (β) sympathetic nerve fibers distributed along the venules of the FL that were near the spinal canal surface (SPG × 400); (D) Cluster and linear sympathetic nerve fibers (strong fluorescence) with some wary sympathetic nerve fibers through the LF nerves were observed in the section of LF (SPG × 400); (E) The fluorescent expression of cadaver specimens is less than that of biopsy specimens, but sympathetic nerve fibers can still be observed around the microarteries in the LF (SPG × 400); (F) The linear (α) and wavy (β) sympathetic nerve fibers were observed in the cadaver specimens, and their measurement widths were also different.(SPG × 400).

TABLE 1 Chi-square test on sections grouped by the direction of sections

	Biopsy specimens					Cadaveric specimens				
	N	Positive+	Negative-	*P-value*	x^2	N	Positive+	Negative-	*P-value*	x^2
Coronal	170	133(78.24)	37 (21.76)	0.192	1.705	229	128(55.90)	101(44.10)	0.348	0.879
*Sagittal	232	52 (22.41)	180(77.59)			160	34 (21.25)	126(78.75)		
Axis	195	141(72.31)	54 (27.69)			210	108(51.43)	102(48.57)		

* Comparisons between each group, $P > 0.05$.; Note: Since background fluorescent of LF fiber at sagittal section was too strong to influence the observation and statistics, the obtained data were not used for statistics for the bigger error.

TABLE 2 Positive and negative sections of the biopsy specimens group and the cadaveric specimens group

	N	Postive+(%)	negative- (%)	*P-value**	x^2
Biopsy specimens group	365	274 (75.07)	91 (24.93)	0.000	39.018
Cadaveric specimens group	439	236 (53.76)	203 (46.24)		

* Comparisons between each group, $P > 0.05$.

TABLE 3 Measurement results of two kinds of nerve fibers

	N	Linearα (μm)	Wavy β (μm)	*x*	*P-value*
Area I	20	0.81 ± 0.04	1.03 ± 0.09	0.92	0.28
Area II		0.73 ± 0.09	1.02 ± 0.07	0.87	

Analysis on Positive Fluorescence Rate of Sections at Different Directions in Human Cervical Ligamentum Flavum (LF)

Because the fluorescence interference of ligament fibers is stronger in the sagittal position, they are not included in the statistics, and the statistics of the positive rate of fluorescence expression on different sections of the two groups are shown in the table (Table 1).

In the biopsy specimen group (experimental group), 170 slices were cut out at the coronal position, and 133 were positive for fluorescent expression, with a positive rate of 78.24%; 195 slices were cut at the axial position, 141 were positive for fluorescent expression, and positive for fluorescent expression. The rate was 72.31%. There was no statistically significant difference in the positive rate of fluorescence expression observed at different positions in the experimental group ($\chi^2 = 1.705$, $P > 0.05$).

In the cadaver specimen group (control group), 229 slices were cut out in the coronal position, and 128 were positively expressed in fluorescence (Fig 7E,F), the positive rate of fluorescence expression was 55.9%; 210 slices were cut out in the axial position, 108 were positively expressed in fluorescence, and the fluorescence expression was positive, The rate was 51.43%. There was no statistically significant difference in the positive rate of fluorescence expression observed in different positions of the control group ($\chi^2 = 0.879$, $P > 0.05$).

There were 365 effective slices in the experimental group, with 274 positive fluorescent expressions, and the positive rate of fluorescence expression was 75.07%. In the control group, there were 439 effective slices, with 236 positive fluorescent expressions, and the positive rate of fluorescence expression was 53.76%. There was a statistical difference between the two groups ($\chi^2 = 39.018$, $P < 0.05$). The positive rate of fluorescent expression in the experimental group was 21.31% higher than that in the control group.

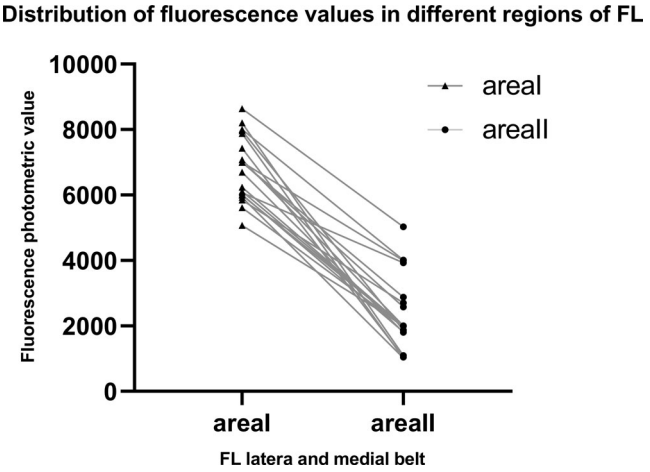

Fig. 8 Comparative statistics of the expression of sympathetic nerve flfluorescence in the LF area I and II, more and denser sympathetic nerve fifibers were distributed in area I compared to area II.

TABLE 4 Comparison of ^{1}HNMR measured values of vertebral canal and dorsal tissues of LF

	N	Lac/Cr	PG/Cho	Cho/Cr	GABA*
LF back	15	1.52 ± 0.46	7.75 ± 1.24	1.01 ± 0.07	0.67 ± 0.09
LF spinal canal		0.97 ± 0.21	11.38 ± 1.03	0.96 ± 0.04	1.29 ± 0.12
t value		4.213	8.721	2.402	16.01
P value		0.000	0.000	0.023	0.000

*The content of GABA in peripheral nerves is very low, and the content of ingredients is more sensitive to NMR testing. The monomer content (non-comparative value) can be used as a reference. LF, ligamentum flavum.

And the existence of nerve fibers was more likely to be observed in biopsy specimens of the experimental group than in cadaver specimens of the control group (Table 2).

Measurement and Analysis on Fluorescence Value in Different Areas (Area I and II) of Human Cervical Ligamentum Flavum (LF)

Twenty sections were randomly selected from a total of 261 sections with positive expression. Based on analysis on fluorescence value of fluorescence units in area I and II of the whole section and image analysis, it is found that the median of area I fluorescence photometric value is 6845, the median of area II fluorescence photometric value is 1994. In turn, area I is 70.87% (4851/6845) higher than the median of area II in fluorescent photometric value, and more and denser sympathetic nerve fibers were distributed in area I compared to area II ($W = 210$, $P < 0.05$). The difference was statistically significant (Fig.8). Two different forms of nerve fibers were measured, as shown in Table 3 and Fig. 7E,F. This shows sparse SPG-stained fibers on coronary sections of area I and II.

Measurement on Width Value of Fluorescence Units of Two Types of Nerve Fibers

The observed sympathetic nerve fibers were measured for their width and the results were concentrated between 0.5 and 1.0 um. All the nerve fibers were C type, similar to the nerve fibers of PLL in morphological characteristics and classification[13], but different in distribution. β type sympathetic nerves were mainly distributed around the capillaries, and, at the same time, α and β sympathetic nerve fibers intersected through LF. Occasionally, α and β sympathetic nerve fibers may be seen among LF in clusters.

Measurement of α and β nerve fiber width expressed in groups area I and area II is expresesd in Table 3. This shows that α nerve fiber widths were in the range from 0.64 to 0.85 um ($x = 0.770$, $\sigma = 0.057$). The β nerve fiber widths were in the range from 0.94 to 1.12 μm ($x = 1.025$, $\sigma = 0.007$). The value of nerve fiber width in area I is 0.920 ± 0.16 um; the value of nerve fiber width in area II is 0.875 ± 0.21 um. The differences between area I and area II were not statistically significant ($t = 1.078$, $P > 0.05$). The differences between the α and β nerve fibers were statistically significant ($t = 6.326$, $P < 0.05$) as β nerve fibers are 25.24% (0.26/1.03) thicker than α fibers on average.

^{1}H NMR Measurement of Metabolites of Nerve Fibers in Ligamentum Flavum (LF)

The obtained ^{1}HNMR spectra from two different locations of the LF (spinal canal/back) can be used to obtain metabolites (Fig. 4A,B). The LF back integral value of each metabolite is as follows: Cho 8.15 ± 0.64, Cr 8.09 ± 0.58, GABA 0.67 ± 0.09, PG 63.16 ± 1.13, Lac 12.29 ± 0.39. The LF spinal canal integral value of each metabolite is as follows: Cho 9.42 ± 0.43, Cr 9.82 ± 0.51, GABA 1.29 ± 0.12, PG 107.12,±1.02, Lac 9.52 ± 0.25. Analysis shows that the integrals and ratios of the neurofibrillary transmitter structure PG/Cho ($t = 8.721$, $P < 0.05$), GABA ($t = 16.01$, $P < 0.05$) increase in the spinal canal of the LF, the difference was statistically significant, 1.47 and 1.93 times of LF back. The changes of neurotransmitter metabolites Lac/Cr ($t = 4.213$, $P < 0.05$), Cho / Cr ($t = 2.402$, $P < 0.05$) reduction showed a statistically significant difference, 0.64 and 0.95 times of LF back (Table 4).

Cases of Vertebral Artery Dissection

Case 1, female, 32 years old, was admitted to the hospital with "onset headache, dizziness and limb weakness for 3 days." The patient experienced severe headache more than 10 min after a neck massage 3 days ago, without slurred speech, limb weakness, and vertigo, accompanied by nausea, vomiting, limb weakness, and frequent episodes of vertigo, which can be relieved after about 30 minutes. Examination: Muscle strength of limbs, grade 5, bilateral finger–nose test and heel–knee–tibia test are stable, bilateral pathological signs are negative, and meningeal irritation signs are negative; brain CT, MRI, MRA (Fig. 2A,B) have no abnormalities. Digital subtraction angiography (DSA) is given in emergency department examination (Fig. 2C,D). We considered the "V4 segment dissection of right vertebral artery." [21] The patient was given aspirin enteric-coated tablets, clopidogrel tablets combined with anti-platelet aggregation, plus low-molecular-weight heparin sodium anticoagulation therapy. Ten days later, "sympathetic symptoms" were completely relieved and the patient was discharged (Fig. 2E,F). The patient was followed up every 2 months. A total of 12 follow-ups were

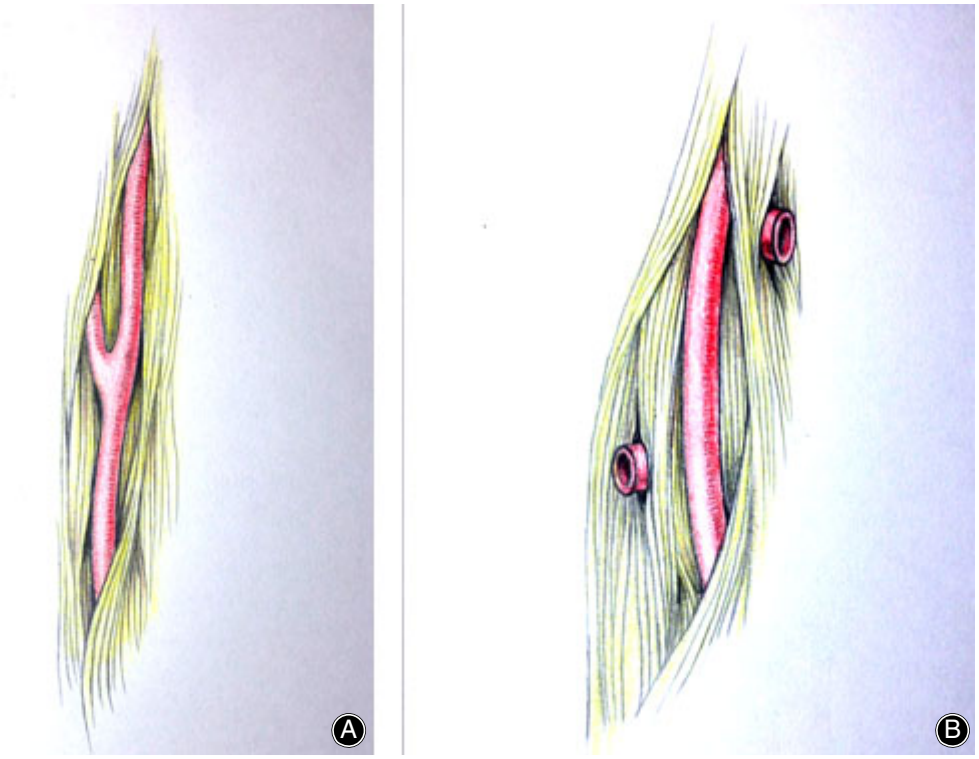

Fig. 9 (A) Schematic diagram of microvascular distribution in LF (along the ligament elastic fibers); (B) Schematic diagram of microvascular distribution in LF (vertical distribution of elastic fibers across ligaments).

carried out within 2 years. The above symptoms occur did not occur after this time.

Case 2, female, 39 years old, "dizzy 4 h" admission, the patient experienced dizziness after neck massage 4 h before admission, accompanied by nausea, vomiting, rapid heartbeat, no limb convulsions and unconsciousness. The attack lasted 3 min, after it could be completely relieved. The above symptoms happened frequently, and the patient then came to the emergency department. There is no abnormality in brain CT and MR (Fig. 3A,B). Examination: heart rate 112 beats/min, lack of consciousness, bilateral pupils and other isosceles, reaction to light exists. The muscle strength and muscle tone of the extremities were normal, and the bilateral Babinski sign was positive. The emergency DSA examination considered the "V3 segment dissection of the right vertebral artery" (Fig. 3C,D). Aspirin was given as well as antiplatelet aggregation and low molecular weight heparin sodium anticoagulant therapy. The "sympathetic symptom" was relieved within 8 days of discharge (Fig. 3E,F) and was followed up for 2 years. A total of 12 follow-up visits were performed in February. The above symptoms did not recur.

Complications

"Sympathetic symptoms" is a systemic syndrome composed of dizziness, headache, rapid heartbeat, palpitation, chest tightness, increased blood pressure, sweating, sleep dysfunction, and other symptoms. Among the cervical spine-related diseases, "vertigo" is more common. The characteristics of the seizures are: the duration of the seizure is short, the time of the seizure is indefinite, the seizure is frequent, and the digestive system is involved. The two rare cases are mainly "vertebral artery dissection," which is easy to diagnose with the "vertebral-basal artery circulation." "Dysfunction" is confused and the difference is the frequency of "sympathetic symptoms" and the prognosis of treatment. Most of the "sympathetic symptoms" after "anticoagulation and antiplatelet" treatment can be effectively relieved, and emergency vascular intervention therapy can also be used. Most of the prognoses are good and stable.

Discussion

Determine the Distribution of Sympathetic Nerve Fibers in the Ligamentum Flavum (LF)

Anatomically, LF is considered to be divided into two parts: intervertebral space and joint capsule. It connects to the joint capsule of the facet joint with extreme fiber at lateral side[22]. Intervertebral elastic fibers are arranged in a rectangular shape from top to bottom, while there is a lack of elastic fibers in the joint capsule. There are venulae in each segment of medial LF close to the midline, which lead to a communion of epidural veins and vertebral vein[23,24].

Through 3D section, SPG staining, and HE staining on human cervical LF, this experiment found distribution of

vascular structure in LF. Structure similar to arteriole goes along elastic fibers of LF of area I near joint capsule, while scattered vessels without arterial wall go among ligament elastic fibers of area I and II. This conforms to the characteristics of anatomical description.

Through analysis on positive fluorescence rate of sections at different directions in the experimental group and the control group (χ^2 = 39.018, $P < 0.05$), sympathetic nerve fibers are distributed in LF.

Distribution Characteristics of Sympathetic Nerve in Ligamentum Flavum (LF)

Sympathetic nerve fibers are mainly C type peripheral sympathetic nerve fibers, which are generally divided into linear type (α) (x = 0.770, σ = 0.057) and wavy type (β) (x = 1.025, σ = 0.007). In coronary sections, more dotted fluorescent units can be observed and there are also linear fluorescent units; while in axial sections, sympathetic nerve fibers with the same direction as ligament fibers are visible. Nerve fibers are basically in the same morphology on different sections, as well as on biopsy specimens (χ^2 = 1.705, $P > 0.05$) and cadaver specimens (χ^2 = 0.879, $P > 0.05$), with homogeneous distribution characteristics.

The distribution density of nerve fibers is decreased from the lateral side (area I) to the medial side (area II) (W = 210, $P < 0.05$). These nerve fibers are mainly distributed in area I near articular capsule and among elastic fibers of ligament in area I and II. The nerve fibers tend to be distributed along the direction of blood vessels (Fig. 5A,B, 6D, and 7A). βfibers are mainly distributed in the peripheral vascular structures, which is similar to the observation on the distribution of sympathetic nerve fibers by Daerr *et al.*[16], that is, the α fibers are scattered among elastic fibers, which can go vertically or horizontally with LF. It is also similar to vascular structures (Figs 5A,B, 6B, and 7A,E). Among ligament elastic fibers, it can be seen sometimes that two kinds of cluster nerve fibers pierce out (Fig. 7D). All these show the close relationship between sympathetic nerve fibers of LF and adjacent structures.

NMR ^{1}H Spectrum Metabolite Distribution Significance

Further ^{1}HNMR analysis of the spinal canal and back of the LF confirmed the presence of sympathetic nerves on the LF. Lac/Cr (t = 4.213, $P < 0.05$) and Cho/Cr (t = 2.402, $P < 0.05$) both increased on the LF back, representing the distribution of vascular-dependent sympathetic nerve fibers[25]. Both PG/Cho (t = 8.721, $P < 0.05$) and GABA (t = 16.01, $P < 0.05$) are considered and show that the content of polysaccharide in the lamina of LF is lower than that in the back; that is, the elastic fibers are cross-linked and loose and easy to cross the blood vessels, while the sympathetic nerves are densely distributed on the LF spinal canal, and their metabolites are active[26]. This information is helpful to indirectly understand the characteristics of sympathetic nerve distribution in LF.

Connections among Ligamentum Flavum (LF), Microvessels, and Sympathetic Nerves

Since LF is a kind of elastic protein connective tissue, changes in movement mean that the relation between elastic fibers also changes correspondingly: thinner at anteflexion and thicker at posterior extension[17,27]. LF consists of elastic fibers, and this experiment shows that the cervical LF suffers the minimum stress and has the maximum strain value[28]. Vessels among the LF elastic fibers were mainly divided into the vessels parallel to LF fibers (Fig. 9A) and those that cross or are perpendicular to the fibers (Fig. 9B). Studies have confirmed that a small force, such as spinal flexion and rotation, or certain coordinated movement, may lead to the rupture of tiny and thin-walled capillaries regularly distributed in degenerated LF[29–32]. It is also reported that stress, conducted by epidural venous plexus and ventral LF, may also cause deformation and even rupture of capillaries in LF[33].

All these findings suggest the mechanical relationship between the movement of LF and the blood vessels inside. Thus, we deduce that regardless of what deformation of LF is, vessel wall through or along the ligament all suffer an axis shear force caused by the relative movement of LF. And these shear forces also act on the vessel wall or sympathetic nerve fibers distributed among elastic fibers of ligaments, thus forming a certain tension and resulting in extension stimulation on sympathetic nerves. In addition, β type fibers in blood vessel wall can also receive this kind of stimulation, which may be linked to vascular structure. However, there still lacks direct measurement evidence for the existence of this force.

The Relationship Between Vertebral Artery Dissection and Sympathetic Symptoms

The rare case of vertebral artery dissection (Figs 2 and 3) we have observed in clinic seems to explain the relationship between blood vessel and nerve at the clinical level. This young patient had no symptoms of vertigo and sympathetic neurosis before onset. After neck massage, he suddenly twisted his neck and developed vascular disease. Angiopathy was detected by emergency DSA examination. The main clinical manifestations of vascular lesions found by emergency admission and DSA examination were paroxysmal vertigo. The time of attack was significantly correlated with neck activity. The vertigo disappeared after anticoagulation treatment. The outpatient follow-up was 2 years and the disease was evaluated to be cured. This can prove that there is a certain connection between blood vessels and nerves and the influence of mechanical action on them cannot be ignored.

The Theory of "Cervical Instability-Sympathetic Nerve-Vertebral Basilar Artery Stimulation"

Some scholars believe that sympathetic nerve excitability is increased in their study on cervical instability[6]. One study also put forward that dizziness caused by injury of proprioceptor in cervical facet joint and deep muscles due to cervical lesions[34] can anatomically remark cervical instability induced

by various soft tissue lesions around cervical vertebrae. Irritated by cervical mechanical instability, sympathetic nerve fibers of these tissues generate an abnormal excitement, which directly acts on capillaries or is received by cervical ganglia and then increases the excitability of sympathetic nerve fibers in vertebral artery. This kind of continuous stimulation causes vertebral artery contracture that affects blood supply and results in cervical vertigo or other kinds of sympathetic nerve symptoms, namely sympathetic nervous cervical spondylosis. This information forms the current "sympathetic nerve theory" and "vascular compression stimulation theory"[35], but these do not integrate various factors to systematically understand the complex causes of "cervical vertigo."

Actually, during human cervical activities, cervical intervertebral disc, zygapophyseal joint, ligaments around vertebral canals, peripheral ligaments, and muscle system all play an important role in assisting dynamic changes. Ligaments around vertebral canals in particular are the key connective tissue structure that maintains the stability of the vertebral body system. All these tissues are confirmed by the existence of the sympathetic nerve fibers, with their own morphological and distribution features. Cervical instability is characterized by "broken"cervical physiology curve on flexion–extension radiographs in clinical. This reflects that the activities of intervertebral joint including flexion and extension are beyond the natural range, which is the manifestation of the cervical degenerative[36]. This is direct evidence put forward by the theory of "cervical instability-sympathetic nerve-vertebral basilar artery stimulation," which can be used to further explore the potential links between cervical biomechanics, anatomy, and pathophysiology.

Limitations

This experiment still has some deficiencies in terms of the accuracy of quantitative analysis. Also, there are a lack of studies on specimens with totally normal anatomic structure under physiological state. Clinically, corresponding sympathetic symptoms not all appear under cervical instability. Therefore, the related research system of cervical spine instability and sympathetic irritability still needs to be established to perfect the theory.

Conclusion

There are sympathetic nerve fibers in human cervical LF. These nerve fibers may be the pathophysiological basis of sympathetic nervous cervical spondylosis.

Supporting Information

Additional Supporting Information may be found in the online version of this article on the publisher's web-site:

Appendix S1. The effect of sympathetic factor on the blood flow of vertebral-basal artery.
Appendix S2. Distribution of sympathetic nerve on the wall of vertebral artery and its correspondence to cervical sympathetic ganglia.
Appendix S3. The abnormality of cervical physiological curvature and pathogenesis cervical spondylotic myelopathy.

References

1. Cooper NA. Dizziness is not diagnostic. BMJ, 2007, 334: 600.
2. Pearce JMS. Barré-Liéou "syndrome". J Neurol Neurosurg Psychiatry, 2004, 75: 319.
3. Ebraheim NA, Lu J, Biyani A, Brown JA, Yeasting RA. Anatomic considerations for uncovertebral involvement in cervical spondylosis. Clin Orthop Relat Res, 1997, 334: 200-206.
4. Wang XW, Gu T, Yuan W. Treatment and mechanism of cervical spondylosis with sympathetic symptoms. Chin J Surg, 2008, 46: 1424–1427.
5. Li Y, Peng B. Pathogenesis, diagnosis, and treatment of cervical vertigo. Pain Physician, 2015, 18: E583–E595.
6. Brandt T, Bronstein AM. Cervical vertigo. J Neurol Neurosurg Psychiatry, 2001, 71: 8–12.
7. Yu TB, Xia YJ, Zou BW. Effect on the blood flow of vertebral basal artery after stimulating the cervical sympathetic ganglions of rabbits. Chin J Spine Spinal Cord, 2000, 10: 157–159.
8. Rao RD, Currier BL, Albert TJ, *et al*. Degenerative cervical spondylosis: clinical syndromes, pathogenesis, and management. J Bone Joint Surg Am, 2007, 89: 1360–1378.
9. Ahmed M, Bjurholm A, Krcicbergs A, Schultzberg M. Tyrosine hydroxylase and vasoactive intestinal polypeptide: immunoreactive nerve fibers in the vertebral bodies, discs, duramater, and spinal ligaments of the rat lumbar spine. Spine, 1993, 18: 268–273.
10. Yu TB, Xia YJ. Distribution of sympathetic nerve on the wall of vertebral artery and its correspondence to cervical sympathetic ganglia. Med J Qilu, 2003, 18: 13–17.
11. Johnson GM. The sensory and sympathetic nerve supply within the cervical spine: review of recent observations. Man Ther, 2004, 9: 71–76.
12. Ohtori S, Takahashi K, Chiba T, Yamagata M, Sameda H, Moriya H. Sensory innervation of the cervical facet joints in rats. Spine, 2001, 26: 147–150.
13. Li H, Ma X, Wu X, *et al*. Morphological observation of sympathetic nerve fibers in the human posterior longitudinal ligament. Spine, 2014, 39: 2119–2126.
14. Cavanaugh JM, Kallakuri S, Ozaktay AC. Innervation of the rabbit lumbar intervertebral disc and posterior longitudinal ligament. Spine, 1995, 20: 2080–2085.
15. Imai S, Konttinen YT, Tokunaga Y, Maeda T, Hukuda S, Santavirta S. An ultra-structural study of calcitonin gene-related peptide-immunoreactive nerve fibets innervating the rat posterior longitudinal ligament. Anlolphologic basis for their possible efferent actions. Spine, 1997, 22: 1941–1947.
16. Daerr M, Allmendinger L, Höfner G, Wanner KT. Synthesis and biological evaluation of fluorescent GAT-ligands based on asymmetric substituted BODIPY dyes. Med Chem Res, 2020, 29: 767–782.
17. Sakamaki T, Sairyo K, Sakai T, Tamura T, Okada Y, Mikami H. Measurements of ligamentum flarum thickening at lumbar spine using MRI. Arch Orthop Trauma Surg, 2009, 129: 1415–1419.
18. Yamada H, Honda T, Yaginuma H, Kikuchi S, Sugiura Y. Comparison of sensory and sympathetic innervation of the dura mater and posterior longitudinal ligament in the cervical spine after removal of the stellate ganglion. J Comp Neurol, 2001, 434: 86–100.
19. Yoon SP, Kim HJ, Choi YS. Anatomic variations of cervical and high thoracic ligamentum flavum. Korean J Pain, 2014, 27: 321–325.
20. Stefan D, Cesare FD, Andrasescu A, *et al*. Quantitation of magnetic resonance signals: the jMRUI software package. Meas Sci Technol, 2009, 20: 251–252.
21. Markus HS, Levi C, King A, Madigan J, Norris J, for the Cervical Artery Dissection in Stroke Study (CADISS) Investigators. Cervical artery dissection in stroke study (CADISS) investigators. Antiplatelet therapy vs anticoagulation therapy in cervical artery dissection: the cervical artery dissection in stroke study (CADISS) randomized clinical trial final results. JAMA Neurol, 2019, 76: 657–664.
22. Aljuboori Z, Boakye M. The natural history of cervical spondylotic myelopathy and ossification of the posterior longitudinal ligament: a review article. Cureus, 2019, 11: e5074.
23. Thompson C, Gonsalves JF, Welsh D. Hyperextension injury of the cervical spine with central cord syndrome. Eur Spine J, 2015, 24: 195–202.

24. Okuda T, Shiotani S, Hayakawa H, Kikuchi K, Kobayashi T, Ohno Y. A case of fatal cervical discoligamentous hyperextension injury without fracture: correlation of postmortem imaging and autopsy findings. Forensic Sci Int, 2013, 225: 71–74.
25. Malik GK, Pandey M, Kumar R, Chawla S, Rathi B, Gupta RK. MR imaging and in vivo proton spectroscopy of the brain in neonates with hypoxic ischemic encephalopathy. Eur J Radiol, 2002, 43: 6–13.
26. Holshouser BA, Ashwal S, Shu S, Hinshaw DB. Proton MR spectroscopy in children with acute brain injury: comparison of short and long echo time acquisitions. J Magn Reson Imaging, 2000, 11: 9–19.
27. Woodworth DC, Holly LT, Mayer EA, Salamon N, Ellingson BM. Alterations in cortical thickness and subcortical volume are associated with neurological symptoms and neck pain in patients with cervical spondylosis. Neurosurgery, 2019, 84: 588–598.
28. Yoganandan N, Kumaresan S, Pintar FA. Geometric and mechanical properties of human cervical spine ligaments. J Biomech Eng, 2000, 122: 623–629.
29. Gazzeri R, Canova A, Fiore C, Galarza M, Neroni M, Giordano M. Acute hemorrhagic cyst of the ligamentum flavum. J Spinal Disord Tech, 2007, 20: 536–538.
30. Hirakawa K, Hanakita J, Suwa H, *et al*. A posttraumatic ligamentum flavum progressive hematoma: a case report. Spine, 1976, 25: 1182–1184.
31. Mahallati H, Wallace CJ, Hunter KM, Bilbao JM, Clark AW. MR imaging of a hemorrhagic and granulomatous cyst of the ligamentum flavum with pathologic correlation. Am J Neuroradiol, 1999, 20: 1166–1168.
32. Mizuno J, Nakagawa H, Inoue T, *et al*. Ligamentum flavum hematoma in the lumbar. Spine; case report. Neurol Med Chir (Tokyo), 2005, 45: 212–215 (in Swedish).
33. Minamide A, Yoshida M, Tamaki T, Natsumi K. Ligamentum flavum hematoma in the lumbar spine. J Orthop Sci, 1999, 4: 376–379.
34. Grgić V. Cervikogena proprioceptivna vrtoglavica: etiopatogeneza, klinicka slika, dijagnostika i terapija s posebnim naglaskom na manualnu terapiju [Cervicogenic proprioceptive vertigo: etiopathogenesis, clinical manifestations, diagnosis and therapy with special emphasis on manual therapy]. Lijec Vjesn, 2006, 128: 288–295 (in Croatian).
35. Wang Z, Wang X, Yuan W, Jiang D. Degenerative pathological irritations to cervical PLL may play a role in presenting sympathetic symptoms. Med Hypotheses, 2011, 77: 921–923.
36. Wang P, Guo SB, Zhang YX, *et al*. The abnormality of cervical physiological curvature and pathogenesis of cervical spondylotic myelopathy. Chinese. J Orthop, 1996, 15: 667–669.